

Sensitivity Analysis of a Numerical High-Frequency Impedance Model for Rotating Electrical Machines

Jose E. Ruiz-Sarrío, *Student Member, IEEE*, Fabien Chauvicourt *Member, IEEE* and Claudia Martis, *Senior Member, IEEE*

Abstract—The prediction of the high-frequency impedance response in rotating electrical machines is utilized to forecast undesired phenomena such as electromagnetic interference and leakage currents. This can be achieved in pre-prototyping design stages by building an equivalent circuit of the machine winding and estimating its parameters numerically. The main objective of this type of model is to predict the trends that the impedance curves will follow if changes on the machine design take place. This article analyzes the effect of the model input parameters on the impedance curves in the two main propagation modes. In addition, the impact of the slot geometry, material characteristics and the winding connection is studied.

Index Terms—AC machines, electromagnetic interference, finite element method, sensitivity analysis

I. INTRODUCTION

Variable frequency drives are commonly used to obtain the controlled operation and supply of rotating electrical machines. The switching harmonics and the voltage gradients (dv/dt) that characterize these devices are the source of undesired high-frequency phenomena such as Electromagnetic Interference (EMI), bearing currents and machine terminal over-voltages [1]. These phenomena are attracting increased attention because of the adoption of wide band-gap semiconductor devices, which provide increased efficiency and performance but operate at increased switching frequencies and voltage gradients [2], [3]. Predictive methods to forecast high-frequency phenomena are commonly utilized in electrical drives. These include models of the power electronics, the cabling and the rotating electrical machine [4]–[6]. The machine model plays a key role on the full drive simulation and its response when excited with high-frequency signals has been studied in the past by several researchers. The most common approach is to emulate the broadband impedance response obtained experimentally by using an

This work has been done in the frame of the European Industrial Doctorate on Next Generation for sustainable Automotive Electrical Actuation (INTERACT) project which has received funding from the European Union Horizon 2020 research and innovation programme under grant agreement No 766180.

Jose E. Ruiz-Sarrío is with the Department of Electrical Machines and Drives, Technical University of Cluj-Napoca, Cluj-Napoca, Romania and Siemens Industry Software NV, Leuven, Belgium (e-mail: Jose.Ruiz@emd.utcluj.ro).

Fabien Chauvicourt is with Engineering Services RTD, Siemens Industry Software NV, Leuven, Belgium

Claudia Martis is with the Department of Electrical Machines and Drives, Technical University of Cluj-Napoca, Cluj-Napoca, Romania

Impedance Analyzer or an LCR meter [7]–[9]. A different approach to model the broadband motor impedance is to utilize numerical methods and equivalent circuits. The most utilized approach to extract the equivalent circuit parameters is the Finite Element Method (FEM). The advantage of this method lays on its early stage capabilities since no motor prototype is a priori needed to build the model. Maki et al. presented a model that utilized a 3D approach to estimate the equivalent circuit parameters with limited accuracy and high computational burden [10]. Other authors attempted to build numerical broadband impedance models utilizing simplified machine prototypes [11], [12]. Heidler et al. developed an induction motor impedance model where frequency dependent effective permeability was utilized to improve the accuracy and efficiency of the resistive and inductive parameters [13]. In [14] a model exclusively utilizing the machine cross-section, conductor distribution and material characteristics was presented and validated. The latter model allows the early-stage broadband impedance estimation with no need of experimental tuning.

This work analyzes the impact of early-stage design decisions on the high-frequency impedance response for the two main propagation modes. The adopted methodology is described in [14]. The sensitivity analysis is performed to test the model capabilities and to provide a better understanding of its application. Section II briefly describes the modeling approach and its main outputs, Section III analyzes the direct effect of the RLC parameters variation on the impedance curves, Section IV studies the connection influence, Section V analyzes the impact of some geometrical parameters and Section VII presents the conclusions extracted from the sensitivity analysis.

II. EARLY-STAGE BROADBAND IMPEDANCE MODELLING STRATEGY

The utilized methodology is based on the coupling of different FEM solvers and a SPICE software. Figure 1 shows a block diagram of the utilized methodology. The equivalent circuit is built according to multi-conductor transmission line theory where each single conductor inside the slots is represented by a lumped pi-equivalent circuit. The parameters of the equivalent circuit are estimated by using two different 2D FEM solvers. An electrostatic solver is utilized to obtain the slot parasitic capacitances, which include the turn-to-ground and inter-turn couplings. The frequency dependent

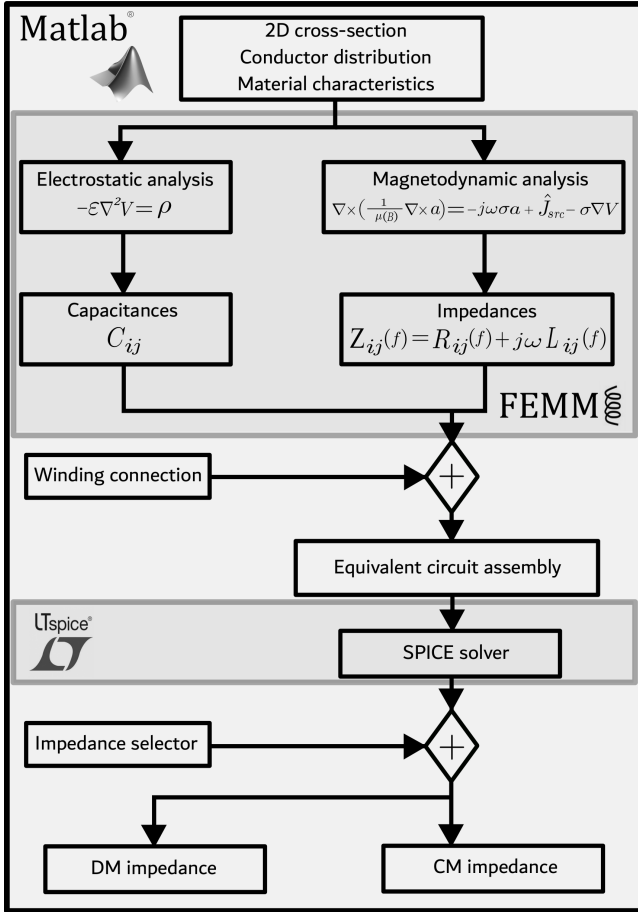


Fig. 1. High-frequency impedance modelling method block diagram

resistances and inductances are estimated by using a magnetodynamic solver. This FEM simulation takes into account the skin and proximity effects in single conductors. In addition, the limited flux penetration due to eddy currents flowing within single laminations is taken into account by utilizing a homogenized iron core model. The frequency dependency of the self- and mutual impedances including the resistive and inductive terms is implemented by using the Laplace transform within SPICE active circuit elements. The equivalent circuit is implemented following the machine stator connections. A general script interfaces the FEM obtained parameters with the SPICE software and extracts the input impedance of the circuit. Further details about the modelling method are presented in [14]–[16].

The case study machine for this work is a 8/12 Permanent Magnet Synchronous Machine (PMSM) with concentrated winding and double layer slots. Figures 2 and 3 depict the machine cross-section and a single tooth geometry respectively. The location of the conductors inside the slot is precisely known for this study, which is one of the main inputs of the model. Methods to determine the conductor distribution even on random wound machines have been developed in the past as shown in [17]. The stator winding connection is formed by star-connecting in series the four coils per phase.

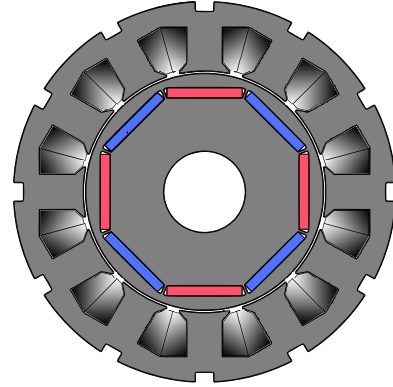


Fig. 2. 8/12 PMSM cross-section depiction

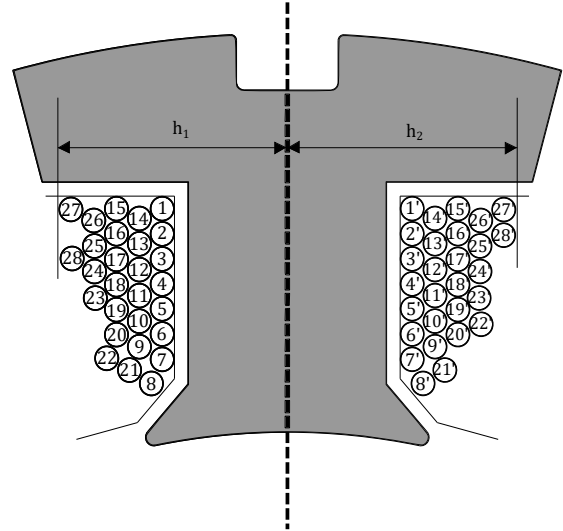


Fig. 3. Single tooth representation

Table I shows the main input parameters for the model.

TABLE I
MODEL INPUT DATA

Copper conductivity	59.6 MS/m
Iron conductivity	2.38 MS/m
Lamination thickness	0.5 mm
Stack length	40 mm
Magnet remanence	1.345 T
BH curve data	M330-50A
Relative permittivity	3.5
Turns/coil	28
Slot wall thickness	0.6 mm
h1 & h2	10.15 mm
Fill factor	0.9
Conductor diameter	1 mm
Conductor insulation	2% of nom. diam.
Winding connection	Series star

The model has been validated experimentally by using an impedance analyzer (Agilent 4294A) with frequency band 40 Hz - 110 MHz. Fixture compensation is performed under open and short circuit conditions. Accuracy starts to decrease from 10 MHz since the parasitics of the leaded test fixture

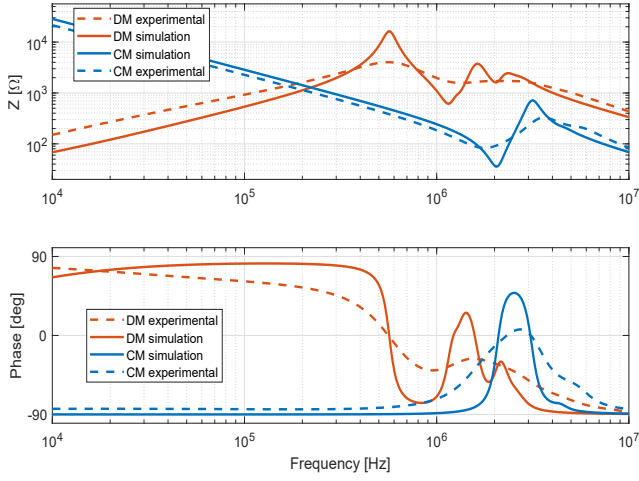


Fig. 4. Comparison between experimental and simulation results

strongly affect the measurements at those frequencies. The connections for impedance measurement are implemented according to the two main propagation modes. The Differential-mode (DM) connection is made between two phases. For the Common-mode (CM) impedance, the connection is made between the machine housing and the three phases in short-circuit. Figure 4 shows the comparison between experimental and simulation results presented in [16].

III. EFFECT OF THE VARIATION OF RLC PARAMETERS

This section analyzes the direct impact of the RLC parameters on the impedance curves. The frequency dependent parameters are modified simultaneously while inter-turn and turn-to-ground capacitances are analyzed separately. Figure 5 shows the effect of the primary parameters variation on the impedance curves for both considered propagation modes. The main effect of the resistance variation in both CM and DM can be noticed in the damping of the resonant points. The damping increases together with the resistance, which is translated on reduced phase and amplitude in the resonance points. The variation of the reactance heavily influences the location of the resonant points, which are shifted towards lower frequencies with increasing reactance for both modes. With increased reactance and constant resistance value, the damping of the resonance also changes. In addition, the amplitude of the DM impedance increases together with the reactance in the frequency range between 10 kHz and 3 MHz when the impedance behaves totally or partially inductive. The effect of the capacitances changes depending on their type. Turn-to-ground capacitances placed in the capacitance matrix diagonal (C_{ii}) affect the two main resonance points in both modes. The greater the turn-to-ground capacitance, the lower the frequency locus of the resonant points. The damping of these points is less affected than for increased reactance values. A strong influence of the turn-to-ground terms is observed in the CM impedance curve, where the amplitude decreases for increased values of these capacitances

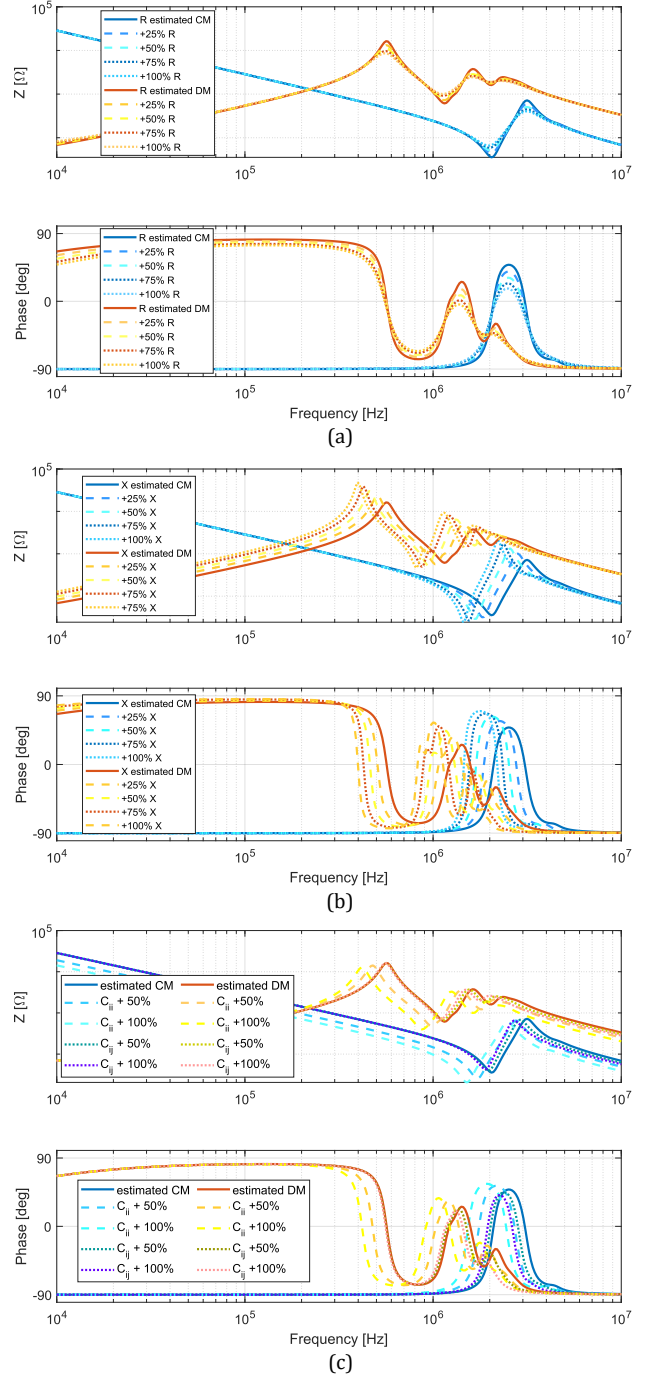


Fig. 5. Effect of RLC parameters variation on the impedance curves, (a) Resistance (R), (b) Reactance (X), (c) Capacitance (C)

over the considered frequency range. Inter-turn capacitances (C_{ij}) located in the off-diagonal entries of the capacitance matrix influence the anti-resonant points located between 1 MHz and 3 MHz for the DM and between 2 MHz and 3 MHz for the CM responses. The main resonant points and impedance amplitudes are not heavily influenced by inter-turn capacitive couplings.

IV. EFFECT OF STATOR WINDING CONNECTION

This section presents the impact of different stator winding connection features. Three simple cases are defined to check the series and parallel connection influence. A single coil, two coils with series connection between them and two parallel branches with two series connected coils are built in the general script. The connection for the CM in the simplified cases is made between the input (P1) and ground. Figure 6 shows the different connections and figure 7 shows the corresponding DM and CM curves. The amplitude in both modes is heavily affected by the connection, having lower and higher values for the CM and the DM curves respectively. The location of the resonant points is mainly affected by the series connection of the coils, while it remains almost unchanged for parallel connections. Thus, it is expected that for a higher number of coils connected in parallel, the frequency of the resonant points will increase.

The turns per coil represents a basic design parameter when assessing the initial machine design. The number of turns in single coils is expected to influence the overall capacitance to ground and the total impedance of the coil. Figure 8 shows the effect of the number of turns per coil on the two impedance curves. For an increased number of turns the amplitude will decrease for the CM curve and increase for the DM one. The resonant frequencies will be shifted towards higher ranges for lower number of turns per coil.

V. EFFECT OF GEOMETRIC PARAMETERS

This section analyzes the impact of some geometric parameters on the impedance curves. The impact of the stack length, conductor diameter and slot wall insulation thickness is evaluated. These parameters will have a direct effect on the capacitance and impedance matrices, which at the same time will influence the impedance curves. The effect on the different RLC parameters is assessed separately.

A. Stack length effect

The stack length adds or reduces the axial length of the conductors within the slots. The utilized methodology is expected to have increased accuracy with larger axial length

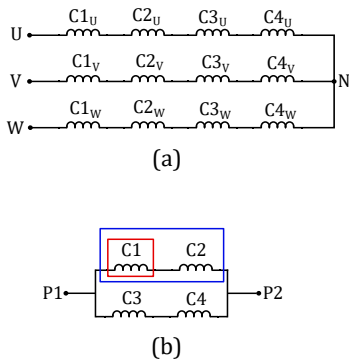


Fig. 6. Stator connection schematic, (a) original connection, (b) simplified connections

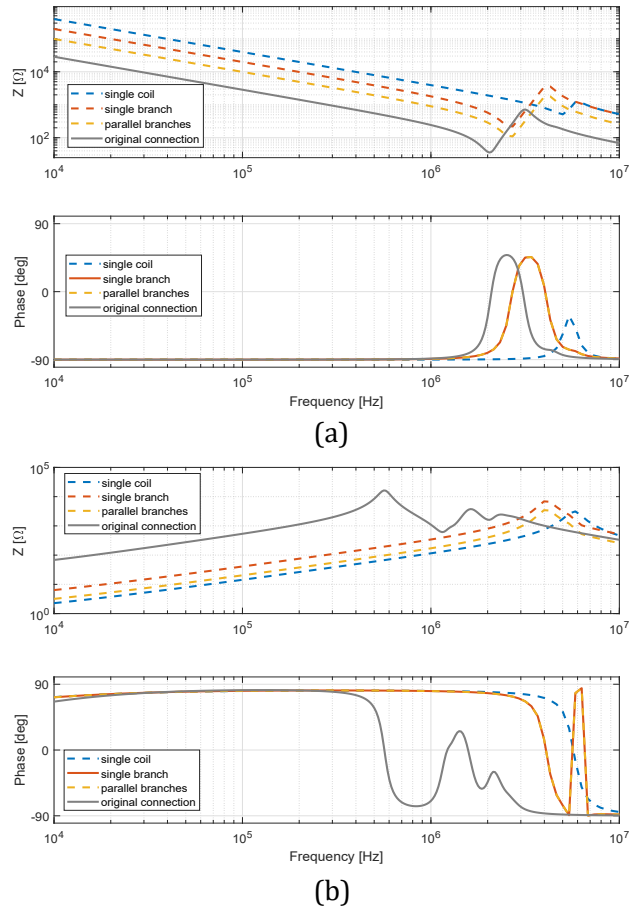


Fig. 7. Impact of winding connection on the impedance curves, (a) CM, (b) DM

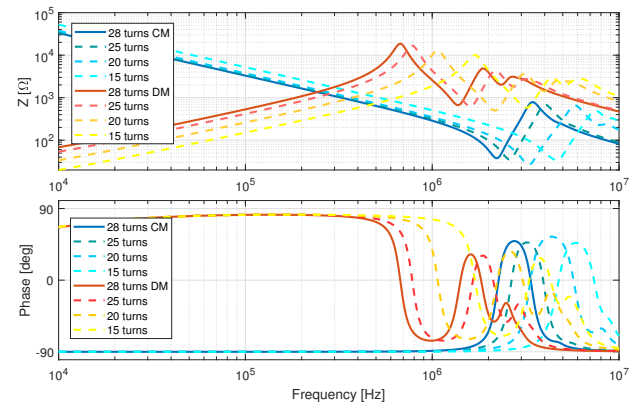


Fig. 8. Impact of the number of turns per coil

since this dimension for large axial lengths greatly overcomes the end-winding extension. However, for increased stack length dimensions it may be necessary to use more than a single lumped-pi equivalent circuit section to properly consider the wave propagation in the conductors. In the present study, only one pi-equivalent section has been considered to address

the stack length variation effect on the RLC parameters and on the impedance curves.

The stack length directly affects the RLC parameters increasing or decreasing their values proportionally. This can be easily deduced since the per unit length values of the RLC parameters are directly multiplied by the conductor length. This dependency is double checked by performing FEM estimations. Figure 9 shows the variation of the real and imaginary parts of the impedance depending on the stack length. Table II shows the variation of parasitic capacitances depending on the stack length. The proportional variation of the RLC parameters causes the impedance curves to shift in phase and amplitude accordingly as shown in figure 10. For increased values of stack length the resonant points are shifted towards lower frequencies in both propagation modes. In addition, the amplitude of the DM and CM impedance curves increases and decreases with the stack length respectively.

TABLE II
STACK LENGTH INFLUENCE ON PARASITIC CAPACITANCES

Stack length [mm]	C_{11} [pF]	C_{12} [pF]	$C_{28'28'}$ [pF]
30	3.13	2.47	0.01
40 (nom)	4.18	3.29	0.010
50	5.22	4.11	0.013
60	6.27	4.93	0.016

B. Conductor diameter effect

This study considers three different conductor diameters, subsequently 1 mm, 0.9 mm and 0.8 mm. This will directly affect the conductor insulation thickness, which directly depends on the size of the conductor. The location of the conductors is not modified since the major objective of the work is to isolate the influence of single modifications. Thus, the coordinate locus of the conductors does not vary. Figure 11 shows the slot geometry for the three considered cases.

The effect of the diameter variation on the self- and mutual impedances is shown in figure 12. The mutual resistances in the lower frequency band (10 kHz - 100 kHz) is the most

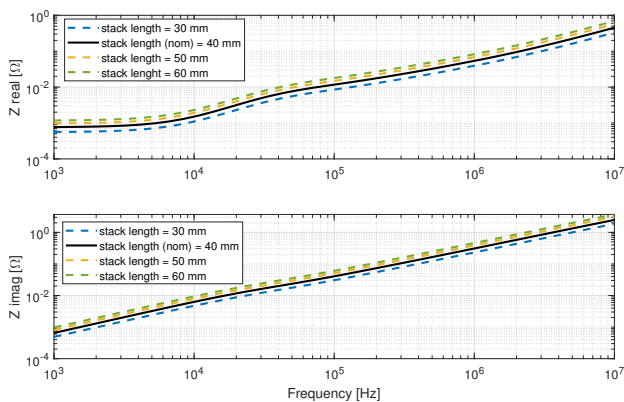


Fig. 9. Impact of the stack length on the self-impedances of conductor 1

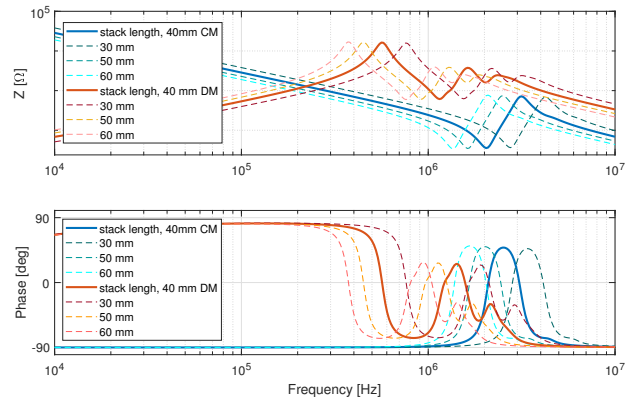


Fig. 10. Impact of the stack length on the DM and CM impedance curves

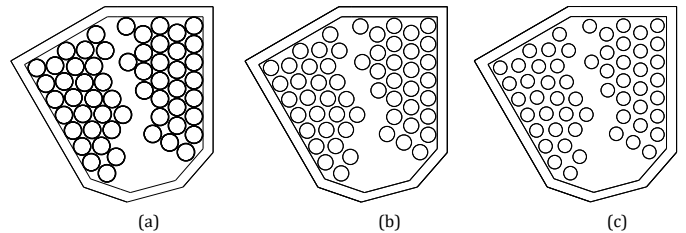


Fig. 11. Slot geometry for different conductor diameter values, (a) 1 mm, (b) 0.9 mm, (c) 0.8 mm

affected parameter. In the range between 100 kHz and 10 MHz the self- and mutual resistances slightly decrease for lower diameter values. Self- and mutual reactances follow similar trends, with slightly higher values for decreased diameter values in the considered frequency range. Regarding parasitic capacitances, the most affected parameters are the inter-turn couplings as shown in Table III. In addition, turn-to-ground capacitances are also affected due to the increased air layer between conductor and insulation. However, the turn-to-ground couplings for conductors not directly facing the slot wall increases. This is caused by the weaker shielding effect that neighboring conductors induce on the electric field distribution. The effect of the conductor diameter variation on the two impedance curves is shown in Figure 13. Both resonant points are shifted towards higher frequencies and less damped. Regarding amplitude values, only the amplitude of the CM curve is notably affected, while the DM curve amplitude in the frequency range between 10 kHz and 400 kHz remains almost unchanged.

TABLE III
CONDUCTOR DIAMETER INFLUENCE ON PARASITIC CAPACITANCES

Conductor diameter [mm]	C_{11} [pF]	C_{12} [pF]	$C_{28'28'}$ [pF]
1 (nom)	4.18	3.29	0.010
0.9	2.51	1.14	0.016
0.8	2.06	0.73	0.022

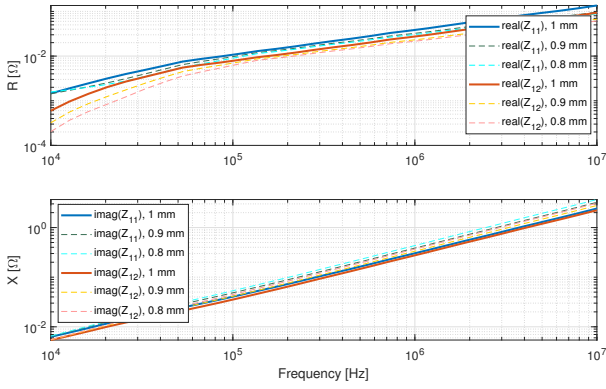


Fig. 12. Effect of the conductor diameter on self (Z_{11}) and mutual (Z_{12}) impedances

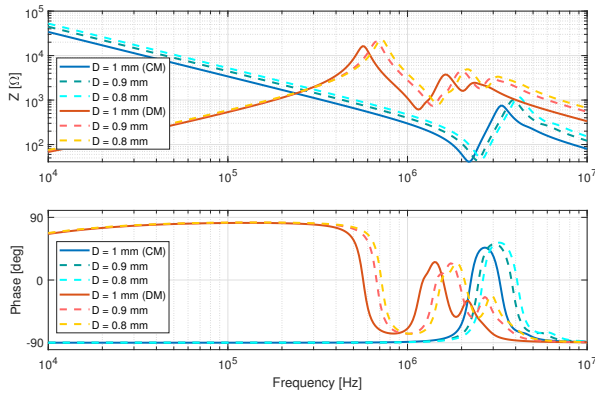


Fig. 13. Impact of conductor diameter on the DM and CM impedance curves

C. Effect of the slot wall insulation thickness

The slot wall insulation has a direct effect on the turn-to-ground capacitances. The conductors are displaced to keep their relative position with respect the insulation. The distance between conductors is also kept constant with exception the conductors in different layers. Figure 14 shows the slot geometry for different values of insulation thickness.

The effect of the insulation thickness on the turn-to-ground capacitances can be observed in Table IV. Four values are analyzed corresponding to conductors located facing the slot wall ($C_{1,1}$), in the second and third rows ($C_{12,12}$, $C_{20,20}$) and conductors in the inner edge of the coil ($C_{28,28}$). The

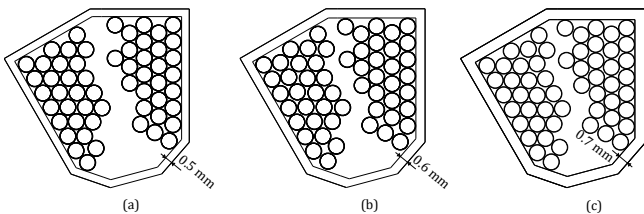


Fig. 14. Slot geometry for different values of slot wall insulation thickness, (a) 0.5 mm, (b) 0.6 mm, (c) 0.7 mm

TABLE IV
SLOT WALL INSULATION THICKNESS INFLUENCE ON PARASITIC CAPACITANCES

Slot wall insulation thickness [mm]	$C_{1,1}$ [pF]	$C_{20,20}$ [pF]	$C_{28,28}$ [pF]
0.5	4.39	0.0028	0.011
0.6 (nom)	4.18	$2.29e-4$	$7.69e-4$
0.7	2.63	$6.94e-5$	$1.37e-5$

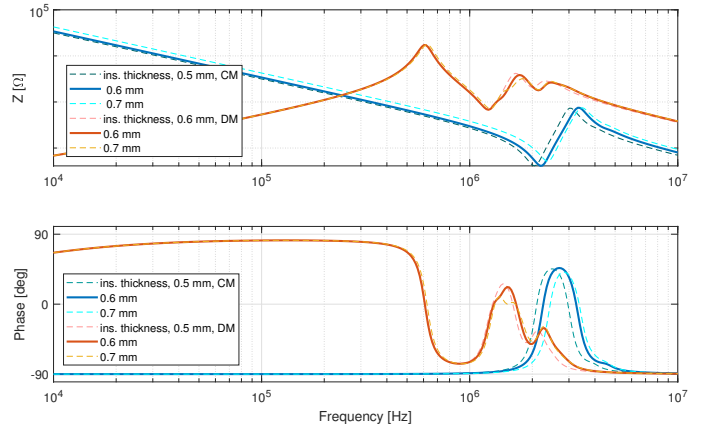


Fig. 15. Impact of slot wall insulation thickness on the DM and CM impedance curves

effect of this variation on the impedance curves is shown in figure 15. From the figure it is possible to observe how the CM curve is influenced by the insulation thickness shifting the resonant point location and affecting the amplitude in the studied frequency range. The DM impedance curve remains unchanged only showing very little variation on the second resonant peak.

VI. CONCLUSION

The present work presented a detailed numerical sensitivity analysis of a high-frequency impedance model applied to a PMSM case study. The aim of this study is to prove the utility of such modelling method on assessing the DM and CM impedance behavior early on the design process of a rotating electrical machine. The method was briefly introduced and the case study PMSM was described. The effect of the RLC parameters was studied in first place, showing the variation of the impedance curves for different values of conductor resistance, inductance and parasitic capacitances. It was proved that the connection of the stator coils has an important effect on the high-frequency impedance as well as the turns-per-coil ratio. In addition, the effect of the most important geometric parameters such as the stack length, conductor diameter and slot wall insulation thickness was studied. The present modelling approach is of use for machine designers pursuing an EMI-aware design since impedance trends can be tracked already at pre-prototyping stages of the rotating electrical machine design. Future work on the topic includes

the experimental measurement of different machine prototypes with different constructional characteristics to check the influence of the various design parameters presented in this work.

REFERENCES

- [1] G. L. Skibinski, R. J. Kerkman, and D. Schlegel, "Emi emissions of modern pwm ac drives," *IEEE Industry Applications Magazine*, vol. 5, no. 6, pp. 47–80, 1999.
- [2] X. Gong and J. A. Ferreira, "Comparison and reduction of conducted emi in sic jfet and si igbt-based motor drives," *IEEE Transactions on Power Electronics*, vol. 29, no. 4, pp. 1757–1767, 2013.
- [3] N. Oswald, P. Anthony, N. McNeill, and B. H. Stark, "An experimental investigation of the tradeoff between switching losses and emi generation with hard-switched all-si, si-sic, and all-sic device combinations," *IEEE Transactions on Power Electronics*, vol. 29, no. 5, pp. 2393–2407, 2013.
- [4] L. Xing, F. Feng, and J. Sun, "Behavioral modeling methods for motor drive system emi design optimization," in *2010 IEEE Energy Conversion Congress and Exposition*. IEEE, 2010, pp. 947–954.
- [5] L. Wang, C. N.-M. Ho, F. Canales, and J. Jatskevich, "High-frequency modeling of the long-cable-fed induction motor drive system using tlm approach for predicting overvoltage transients," *IEEE Transactions on Power Electronics*, vol. 25, no. 10, pp. 2653–2664, 2010.
- [6] B. Revol, J. Roudet, J.-L. Schanen, and P. Loizelet, "Emi study of three-phase inverter-fed motor drives," *IEEE Transactions on Industry Applications*, vol. 47, no. 1, pp. 223–231, 2010.
- [7] A. Boglietti and E. Carpaneto, "Induction motor high frequency model," in *Conference Record of the 1999 IEEE Industry Applications Conference. Thirty-Forth IAS Annual Meeting (Cat. No. 99CH36370)*, vol. 3. IEEE, 1999, pp. 1551–1558.
- [8] B. Mirafzal, G. L. Skibinski, R. M. Tallam, D. W. Schlegel, and R. A. Lukaszewski, "Universal induction motor model with low-to-high frequency-response characteristics," *IEEE Transactions on Industry Applications*, vol. 43, no. 5, pp. 1233–1246, 2007.
- [9] I. Stevanović, B. Wunsch, and S. Skibin, "Behavioral high-frequency modeling of electrical motors," in *2013 Twenty-Eighth Annual IEEE Applied Power Electronics Conference and Exposition (APEC)*. IEEE, 2013, pp. 2547–2550.
- [10] K. Maki, H. Funato, and L. Shao, "Motor modeling for emc simulation by 3-d electromagnetic field analysis," in *2009 IEEE International Electric Machines and Drives Conference*. IEEE, 2009, pp. 103–108.
- [11] N. Boucenna, F. Costa, S. Hlioui, and B. Revol, "Strategy for predictive modeling of the common-mode impedance of the stator coils in ac machines," *IEEE Transactions on Industrial Electronics*, vol. 63, no. 12, pp. 7360–7371, 2016.
- [12] Y. Xie, J. Zhang, F. Leonardi, A. R. Munoz, M. W. Degner, and F. Liang, "Modeling and verification of electrical stress in inverter-driven electric machine windings," *IEEE Transactions on Industry Applications*, vol. 55, no. 6, pp. 5818–5829, 2019.
- [13] B. Heidler, K. Brune, and M. Doppelbauer, "High-frequency model and parameter identification of electrical machines using numerical simulations," in *2015 IEEE International Electric Machines & Drives Conference (IEMDC)*. IEEE, 2015, pp. 1221–1227.
- [14] J. E. Ruiz-Sarrió, F. Chauvicourt, J. Gyselinck, and C. Martis, "High-frequency modelling of electrical machine windings using numerical methods," in *2021 IEEE International Electric Machines & Drives Conference (IEMDC)*. IEEE, 2021, pp. 1–7.
- [15] J. E. R. Sarrió, C. Martis, and F. Chauvicourt, "Numerical computation of parasitic slot capacitances in electrical machines," in *2020 International Conference and Exposition on Electrical And Power Engineering (EPE)*. IEEE, 2020, pp. 146–150.
- [16] J. E. Ruiz-Sarrió, F. Chauvicourt, J. Gyselinck, and C. Martis, "Impedance modelling oriented towards the early prediction of high-frequency response for permanent magnet synchronous machines," *IEEE Transactions on Industrial Electronics - Accepted for final publication (June 2022)*.

Jose E. Ruiz-Sarrió was born in Valencia, Spain in 1992. He received a double M.Sc. in Industrial Engineering and in Electrical Engineering from Universidad Politecnica de Valencia and Politecnico di Milano respectively, in 2018. He is currently a PhD candidate within the Technical University of Cluj-Napoca. Moreover, he is involved in the H2020 MSCA research project INTERACT which includes Siemens Industry Software NV, Leuven, Belgium as an industrial partner in his PhD track. His main research interests include high-frequency phenomena, fault diagnosis and condition monitoring in Electrical Machines and Drives.

Fabien Chauvicourt received his M.Sc. degree (2014) in Mechanical Engineering from the Universite de Technologie de Compiègne, and his double PhD degree (2018) in Mechanical Engineering from the Katholieke Universiteit Leuven, Belgium and in Electrical Engineering from Universit e Libre de Bruxelles, Belgium. He is currently an Advanced Research Engineer within Siemens Industry Software NV focusing his research on model-based engineering (electric powertrain development, multi-physical system-level modelling, virtual integration of component behavior) and datadriven engineering (artificial intelligence, machine learning, signal processing).

Claudia Martis was born in Macin, Romania, in 1967. She started her university studies, in 1985. She graduated in electrical engineering from Polytechnic Institute, Cluj-Napoca, in 1990, and the Ph.D. degree from the Chair of the Electrical Machines, Marketing and Management, Technical University of Cluj-Napoca, under the coordination of Prof. Karoly Agoston Biro, in 2001. Her Ph.D. thesis entitled Contributions to the Study of Doubly-Salient Permanent Magnet Reluctance Machines. After three years working as an Engineer with SINTEROM SA, Cluj-Napoca, she joined the Chair of the Electrical Machines, Marketing and Management, Technical University of Cluj-Napoca, first as an Associate Assistant and has been a full-time Teaching and Research Assistant, since 1996. She is currently a Full Professor with the Department of Electrical Machines and Drives, Faculty of Electrical Engineering, Technical University of Cluj-Napoca.